

PAPER

## spFRET reveals changes in nucleosome breathing by neighboring nucleosomes

To cite this article: Ruth Buning *et al* 2015 *J. Phys.: Condens. Matter* **27** 064103

View the [article online](#) for updates and enhancements.

### You may also like

- [Nucleosome positioning and composition modulate \*in silico\* chromatin flexibility](#)  
N Clauvelin, P Lo, O I Kulaeva et al.
- [A unified computational framework for modeling genome-wide nucleosome landscape](#)  
Hu Jin, Alex I Finnegan and Jun S Song
- [Ubiquitous human 'master' origins of replication are encoded in the DNA sequence via a local enrichment in nucleosome excluding energy barriers](#)  
Guénola Drillon, Benjamin Audit, Françoise Argoul et al.

# spFRET reveals changes in nucleosome breathing by neighboring nucleosomes

Ruth Buning, Wietske Kropff, Kirsten Martens and John van Noort

Huygens-Kamerlingh Onnes Laboratory, Leiden University, Niels Bohrweg 2, 2333 CA Leiden, The Netherlands

E-mail: [noort@physics.leidenuniv.nl](mailto:noort@physics.leidenuniv.nl)

Received 28 May 2014, revised 25 July 2014

Accepted for publication 31 July 2014

Published 7 January 2015



CrossMark

## Abstract

Chromatin, the structure in which DNA is compacted in eukaryotic cells, plays a key role in regulating DNA accessibility. FRET experiments on single nucleosomes, the basic units in chromatin, have revealed a dynamic nucleosome where spontaneous DNA unwrapping from the ends provides access to the nucleosomal DNA. Here we investigated how this DNA breathing is affected by extension of the linker DNA and by the presence of a neighboring nucleosome. We found that both electrostatic interactions between the entering and exiting linker DNA and nucleosome–nucleosome interactions increase unwrapping. Interactions between neighboring nucleosomes are more likely in dinucleosomes spaced by 55 bp of linker DNA than in dinucleosomes spaced by 50 bp of linker DNA. Such increased unwrapping may not only increase the accessibility of nucleosomal DNA in chromatin fibers, it may also be key to folding of nucleosomes into higher order structures.

Keywords: nucleosome, chromatin, spFRET, dynamics

(Some figures may appear in colour only in the online journal)

 Online supplementary data available from [stacks.iop.org/JPCM/27/064103/mmedia](http://stacks.iop.org/JPCM/27/064103/mmedia)

## 1. Introduction

Chromatin consists of arrays of nucleosomes connected with 10–90 base pairs (bp) of linker DNA [25]. Interactions between these nucleosomes lead to dense higher order structures. Although the arrangement of nucleosomes and the DNA trajectory in chromatin has been investigated intensively in the past decades, the structure of chromatin remains highly debated [28]. The compact state of native chromatin under physiological salt conditions was visualized by electron microscopy (EM) more than 35 years ago [21]. The DNA trajectory in the fiber was however not visible in the EM pictures of compacted chromatin. The crystal structure of a tetranucleosome, four nucleosomes connected by 20 bp linker DNA, provides more detailed information on the arrangement of nucleosomes and the DNA trajectory [30]: next-neighbors interact in a face-to-face configuration and the linker DNA is straight. A similar small array, consisting of three nucleosomes connected by 20 bp linker DNA, has been investigated with FRET (fluorescence or Förster resonance energy transfer) [23]. The array compacts under influence of magnesium,

and next-neighbors appear to interact face-to-face in the same way as in the crystal structure, as demonstrated by a high FRET efficiency between the labels on next-neighboring nucleosomes. Recently, this arrangement was confirmed by cryogenic EM of 20 and 30 bp linker DNA chromatin fibers that included linker histones [31].

The interactions between nucleosomes are mediated by electrostatics and specific contacts involving flexible histone tails [15]. The unstructured tails allow for alternative orientations between nucleosome pairs that put different constraints on the linker DNA. In native chromatin, the linker length varies between 10 and 90 bp [25], which may lead to interactions between other nucleosome pairs and hence a different topologies of the chromatin fiber. Indeed, EM experiments on reconstituted nucleosomal arrays with 30–90 bp linker length suggest interactions between direct neighbors [28]. The force-extension behavior of nucleosomal arrays with 50 bp linker length, as measured on single chromatin fibers using magnetic tweezers, also suggests interactions between direct neighbors [18]. From such force spectroscopy experiments, another interesting

feature arises: a large increase in fiber length at a force of 4 pN indicates the disruption of nucleosome–nucleosome interactions [4]. This length increase is larger than what would be expected from the extension of the linker DNA only. The disruption of nucleosome–nucleosome interactions seems to be accompanied by partial unwrapping of the nucleosomal DNA, suggesting that in the condensed fiber, the nucleosomal DNA may already be partly unwrapped.

Partial unwrapping of nucleosomes in a compacted chromatin fiber would have consequences for the accessibility of nucleosomal DNA. It might even make part of the nucleosomal DNA more accessible in a folded chromatin fiber than in an individual nucleosome. Poirier *et al* [22] have investigated the accessibility of nucleosomal and linker DNA to restriction enzymes in both mononucleosomes (MNs) and in nucleosomal arrays. Interestingly, they found that parts of the nucleosomal DNA in a fiber can be up to eight-fold more accessible than in MNs.

Individual nucleosomes are dynamic structures. DNA breathing, the transient unwrapping of DNA from the histone core, makes nucleosomal DNA accessible for DNA-binding proteins [24, 32]. Single-pair, FRET (spFRET) [14] experiments have quantified this [3], revealing DNA breathing from both nucleosome ends. Nucleosomes are open for about 10% of the time for tens of milliseconds [16]. DNA breathing is modulated by DNA sequence and by post-translational modifications to the histone proteins [13, 20]. So far, spFRET experiments have mainly focused on individual nucleosomes, ignoring how nucleosome conformation and dynamics are influenced when the nucleosome is embedded in a chromatin fiber. To address this question, we focus here on (partial) unwrapping of nucleosomal DNA in nucleosomes flanked by linker DNA and/or by a second nucleosome.

We measure unwrapping of nucleosomal DNA in dinucleosomes (DNs) with 50 bp linker length, because this is the average linker length found *in vivo* [25] and commonly used in chromatin fiber experiments [18, 28, 29]. The mechanical properties of the linker DNA pose constraints on the conformational freedom to position nucleosomes face-to-face, and the energy required to bend the linker DNA could be reduced by partial unwrapping of the nucleosomal DNA. We therefore expect that interactions between nucleosomes will be accompanied by DNA unwrapping from the nucleosome exit, in accordance with observations made by force spectroscopy on single chromatin fibers [4].

The energy required to bend the linker DNA depends on sterical constraints as well as on the linker DNA length. Variations of only a few bp have significant effects on the torsional energy required for positioning neighboring nucleosomes face-to-face, due to the 10.4 bp helical periodicity of DNA. Increasing the linker length with 5 bp from 50 to 55 bp is just a 1.7 nm change in length, but changes the relative orientation of two non-interacting nucleosomes by 180° (see figure 2 for an illustration). So far, the effect of the linker length has mostly been studied for multiples of 10 bp. However, a natural preference for  $10n + 5$  bp linker DNA has been suggested, and observed in yeast [2, 34, 35]. Such a ‘phase offset’ may play a crucial role in the formation of chromatin higher order structure.

Not only interactions between nucleosomes determine higher order chromatin structure, the linker DNA itself may also have an effect on the DNA trajectory in the fiber by steric and/or electrostatic interactions with the nucleosome and/or other stretches of linker DNA.

Here, we describe spFRET experiments on single fluorescently labeled nucleosomes flanked by either 300 bp linker DNA or a neighboring nucleosome with 20 or 50 bp linker DNA. Moreover, we compare unwrapping in DNs with 50 and with 55 bp linker DNA. We show that the presence of linker DNA and of a neighboring nucleosome results in a significant change in FRET distribution, depending on the linker length. The presence of linker DNA enhances unwrapping of nucleosomal DNA. In DNs with 55 bp linker DNA, interactions between the nucleosomes appear to further increase the unwrapping probability of the nucleosomal DNA.

## 2. Materials and methods

### 2.1. Preparation of DNA constructs

A 198 bp DNA template containing a single 601 nucleosome positioning sequence was constructed by polymerase chain reaction (PCR). The forward and reverse primers were labeled at a single position with Cy3B and ATTO647N (via amino linker with six-carbon spacer to the base; IBA. Primer sequences can be found in the online supplementary material ([stacks.iop.org/JPCM/27/064103/mmedia](http://stacks.iop.org/JPCM/27/064103/mmedia)). The donor and acceptor were separated by 81 bp. After reconstitution, the donor (Cy3B) is located at the second base pair from the nucleosome exit. The acceptor (ATTO647N) is located 10 bp from the dyad, leading to a FRET efficiency larger than 0.5 for a fully folded nucleosome. The layout of the MN construct is shown in figure 1. Two non-palindromic restriction sites were included close to the DNA ends: BsaI and BseYI, which were subsequently used to build longer constructs by ligation.

After purification, the 198 bp construct was digested with either BsaI or BseYI and ligated to 300 bp DNA without any nucleosome positioning sequence, or DNA with a second, unlabeled, 601 nucleosome positioning sequence. If necessary, the ligated DNA product was purified from agarose gel to remove unligated product. Figure 2 schematically shows all nucleosome constructs described in this paper.

### 2.2. Nucleosome reconstitution

DNA and chicken erythrocyte histone octamers were mixed in various molar ratios in TE (1 mM ethylenediaminetetraacetic acid (EDTA), 10 mM Tris.HCl pH 8.0) and 2 M NaCl. MNs and DNs were reconstituted by salt gradient dialysis against 0.85, 0.65, 0.5 and finally 0 M NaCl, all buffered with TE in a total volume of 40  $\mu$ l and a labeled DNA concentration around 50 nM. Competitor DNA, 147 bp unlabeled random sequence DNA (produced with PCR), was included in the reconstitution reaction at concentrations between 150 and 300 nM.

### 2.3. Polyacrylamide gel electrophoresis

Nucleosome reconstitutions were analyzed with 5% native polyacrylamide gel electrophoresis (PAGE). A sample of

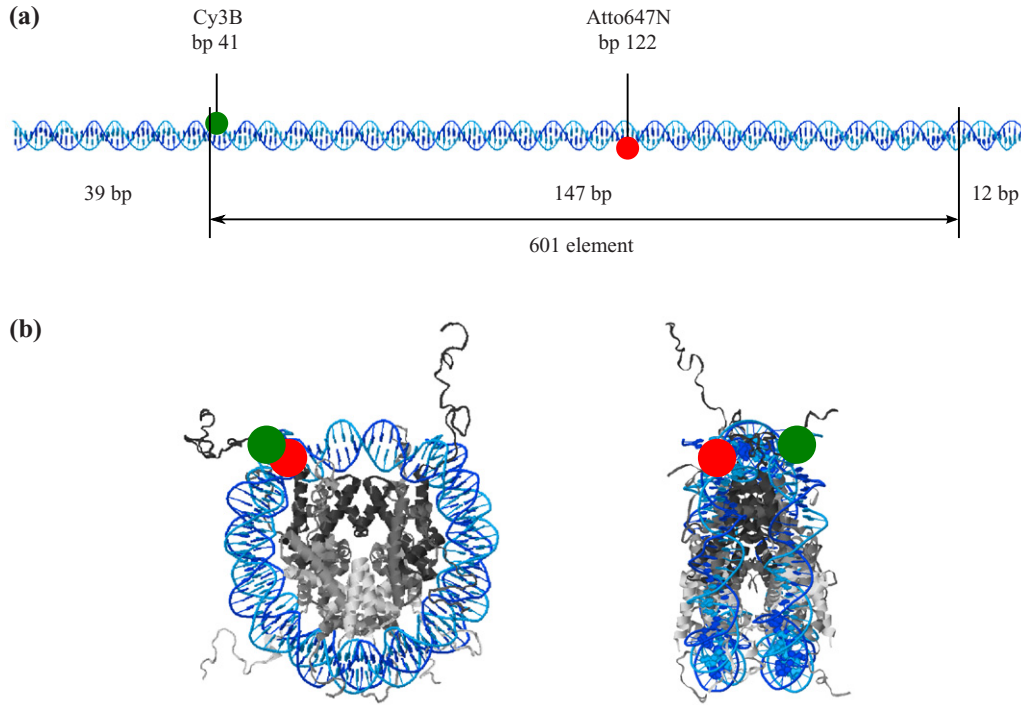


**Figure 1.** (a) The 198 bp DNA construct, indicating the position of the 601 positioning element and the fluorescent labels. (b) Top and side view of the crystal structure of the nucleosome core particle (1KX5) [7], consisting of 147 bp DNA wrapped around the histone octamer. The positions of the fluorescent labels are indicated.

2–8  $\mu\text{l}$  of reconstitution product was loaded on the gel (29 : 1 bis : acrylamide,  $0.2 \times \text{TB}$ , Amersham Bioscience Hoefer SE 400 vertical gel slab unit). The gel was run at  $19 \text{ V cm}^{-1}$  at  $7^\circ \text{C}$  for 90–120 min to separate nucleosomes from free DNA. The fluorescence was imaged with a gel imager (Typhoon 9400, GE Healthcare). Red: excitation at 633 nm, emission detected at 670 nm; Green: excitation at 532 nm, emission detected at 580 nm; FRET: excitation at 532 nm, emission detected at 670 nm (all 30 nm bandpass). Gel images were analyzed with ImageJ software to determine the relative intensities of the bands. The uncorrected proximity ratio ( $E_{\text{PR}}^{\text{raw}}$ ), as a measure for the FRET efficiency in the bands, was calculated according to equation (1).

#### 2.4. Sample preparation

Fluorescently labeled nucleosomes were diluted to a concentration of 50–100 pM in a buffer containing 10 mM Tris.HCl pH 8.0,  $0.1 \text{ mg ml}^{-1}$  BSA, 0.03% Nonidet-P40 and 2 mM trolox. Where stated, 100 mM KAc and 2 mM MgAc<sub>2</sub> were added to the buffer. We used non-stick tubes (Ambion) for nucleosome dilutions. After 15–30 min of equilibration to room temperature, a drop of 50  $\mu\text{l}$  was placed on a glass coverslide (#1.5, Menzel) and imaged as described below.

#### 2.5. Single molecule fluorescence microscopy

Single molecules were imaged with a home-built confocal microscope equipped with a  $60 \times$  water-immersion objective (NA = 1.2, Olympus), as schematically depicted in figure 3(a) (see also [16]). A 515 nm diode pumped solid state laser (Cobolt) and a 636 nm diode laser (Power Technology) were

used as excitation sources. The lasers were alternated at 20 kHz by analog modulation, either directly (636 nm), or with an AOM (515 nm; Isomet). The beams were spatially filtered with a single-mode fiber, and focused 25  $\mu\text{m}$  above the glass–buffer interface by the objective. The excitation power was 13  $\mu\text{W}$  for 515 nm excitation, and 6  $\mu\text{W}$  for 636 nm excitation. The collected fluorescence was spatially filtered with a 50  $\mu\text{m}$  pinhole in the image plane, and was split into a donor and an acceptor channel by a dichroic mirror (640dcsr, Chroma). The fluorescence was filtered with emission filters (hq570/100 m for the donor channel, hq700/75 m for the acceptor channel, Chroma) to minimize crosstalk, and was imaged on the active area of single photon avalanche photodiodes (SPCM AQR-14, Perkin-Elmer). The photodiodes were read out with a TimeHarp 200 photon counting board (Picoquant GmbH). In a typical experiment, data was collected for 30 min in which 2000–10 000 bursts of fluorescence were detected.

#### 2.6. Single molecule data analysis

Bursts of fluorescence were detected using the method described in [9]. A burst was assigned if a minimum of 50 photons were detected with a maximum interphoton time of 100  $\mu\text{s}$ . Photon arrival times in the donor (D) and acceptor (A) channel were sorted according to excitation wavelength, resulting in four photon streams: D-emission upon D-excitation:  $I_{\text{Dex}}^{\text{Dem}}$ , A-emission upon D-excitation:  $I_{\text{Dex}}^{\text{Aem}}$ , D-emission upon A-excitation:  $I_{\text{Aex}}^{\text{Dem}}$ , A-emission upon A-excitation:  $I_{\text{Aex}}^{\text{Aem}}$ . Example data are shown in figure 3(b).

For each burst, we estimated the FRET efficiency by the sensitized-acceptor emission method [6, 8]. Following the

	Elementary Mononucleosome			
	Mononucleosomes with 300 bp linker DNA	Dinucleosomes 20 bp linker DNA	50 bp linker DNA	55 bp linker DNA
linker DNA attached at the label side		—		
linker DNA attached at the opposite side				

**Figure 2.** Schematic overview of the constructs described in this chapter. The elementary MN contains a single 601 element, flanked by 39 bp on the side closest to the fluorescent labels, and by 12 bp on the opposite side. All other constructs are extensions of the elementary nucleosome. The MNs with 300 bp linker DNA contain a single 601 element, flanked by 300 bp either on the label side (MNI300), or on the opposite side (MNo300). The DNs contain two 601 elements, linked by 20, 50 or 55 bp linker DNA. The two 601 elements are linked via the label side (DNI50 and DNI55), or via the opposite side (DNo20, DNo50 and DNo55). DNs linked by 20 bp linker DNA via the label side are missing due to constraints imposed by the positions of restriction sites. The percentages of open nucleosomes ( $E_{PR}^{raw} < 0.3$ ) correspond to single molecule measurements in 100 mM KAc. Structures shown are based on the nucleosomal DNA from the crystal structure of the nucleosome core particle (1KX5) [7], which we extended with linear stretches of DNA with the use of [37]. The histone octamers are left out for visual clarity. Note that the images of the constructs just display a linear extension of the linker DNA, and do not reflect actual experimentally determined or theoretically predicted trajectories of the linker DNA. FRET experiments with both labels on the linker DNA rather suggest that the linker DNA may be bent [33].

definitions described by Lee *et al* [19], we calculated the uncorrected proximity ratio  $E_{PR}^{raw}$  and label stoichiometry  $S^{raw}$  from the total number of photons in the burst for the different photon streams:

$$E_{PR}^{raw} = (I_{D_{ex}}^{A_{em}})/(I_{D_{ex}}^{A_{em}} + I_{D_{ex}}^{D_{em}}) \quad (1)$$

$$S^{raw} = (I_{D_{ex}}^{A_{em}} + I_{D_{ex}}^{D_{em}})/(I_{D_{ex}}^{A_{em}} + I_{D_{ex}}^{D_{em}} + I_{A_{ex}}^{A_{em}}). \quad (2)$$

The excitation powers were chosen such that  $I_{D_{ex}}^{A_{em}} + I_{D_{ex}}^{D_{em}} \approx I_{A_{ex}}^{A_{em}}$  for doubly labeled particles, resulting in  $S^{raw} \sim 0.5$ . An example of a 2D E, S histogram from a typical measurement is shown in figure 3(c). Nucleosomes containing both donor and acceptor fluorophores were selected for further analysis by taking only bursts with  $0.2 < S^{raw} < 0.8$ . Histograms of the FRET efficiencies of these bursts show the distribution of FRET efficiencies of the doubly labeled nucleosomes only. Bursts of two or three measurements of the same construct and conditions were verified for reproducibility and combined to build one FRET histogram. Histograms were normalized to a total area under the curve of 1 to allow comparison of different constructs. The fraction without FRET (representing open or (partly) dissociated nucleosomes) was determined by taking the area below the histogram for  $E_{PR}^{raw} < 0.3$ .

Note that we did not attempt to quantify the extent of DNA unwrapping from the histone core. The limited number

of photons per burst, the complications with the translation from FRET efficiency to label pair distance [19], and the possibility of conformational changes within a single burst prevent a direct calculation of the label pair distance and from that the nucleosome conformation. Alternatively, one can change the positions of the labels along the DNA to resolve the extent of DNA unwrapping [16, 20], but this requires new DNA constructs. By choosing the location of the FRET pair to be at the very end of the nucleosomal DNA, we ensure that all DNA unwrapping events of over 10 bp DNA are captured in our measurements [3]. In this paper, increased unwrapping therefore refers to more frequent breathing rather than breathing of larger stretches of nucleosomal DNA.

### 3. Results

#### 3.1. Gel electrophoresis of (di)nucleosome reconstitutions

Figure 4 shows the fluorescence in (di)nucleosomes after native gel electrophoresis of all reconstituted nucleosomal constructs, separating free DNA from nucleosomes. The amount of free DNA is generally much smaller than the amount of reconstituted nucleosomes, confirming a high reconstitution yield. As opposed to bare DNA, nucleosomes show significant FRET, indicating reconstitution into fully wrapped nucleosomes, properly positioned on the 601 elements.

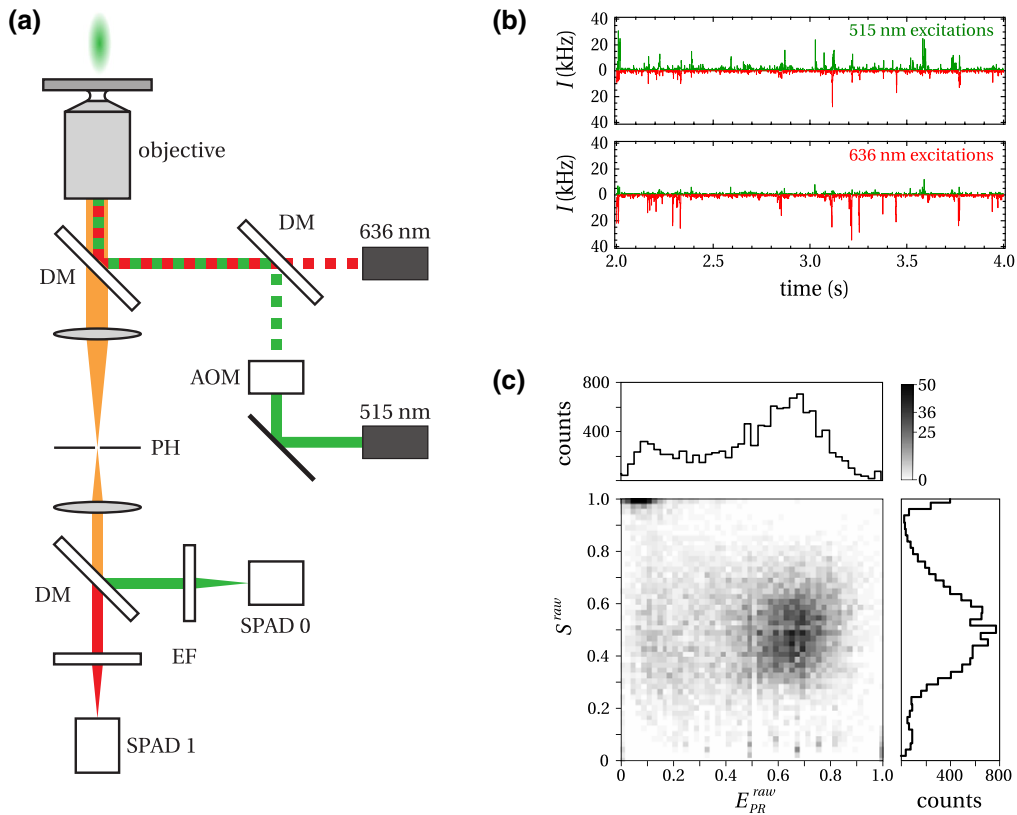


**Figure 3.** (a) Schematic overview of the confocal FRET microscope. DM: dichroic mirror; AOM: acousto-optical modulator; PH: pinhole; EF: emission filter; SPAD: single photon avalanche diode. The dotted red and green lines represent the modulation of the lasers, using a modulation period of  $25 \mu\text{s}$ . (b) Typical intensity timetraces of the four different photon streams acquired with the setup in (a). Photon arrival times are binned to 1 ms. Bursts of fluorescence arise from the passage of a single particle through the excitation volume. (c) Typical 2D-histogram of FRET efficiency ( $E_{PR}^{raw}$ ) and label stoichiometry ( $S^{raw}$ ) for MNs. Four populations are distinguishable: donor only ( $S^{raw} > 0.8$ ), acceptor only ( $S^{raw} < 0.2$ ), doubly labeled ( $0.2 < S^{raw} < 0.8$ ) with FRET ( $E_{PR}^{raw} > \sim 0.3$ ) and without FRET ( $E_{PR}^{raw} < \sim 0.3$ ).

In most cases, a single sharp band of nucleosomes is present. However, sometimes a second band is visible just below the main nucleosome band. This minor band can be attributed to incomplete nucleosomes, lacking the H2A/H2B dimer(s). In all cases there is some material left in the slots, originating from aggregates, that show a small FRET signal as well.

FRET differences between constructs are readily visible in the gel: the FRET efficiency of DN depends on the linker DNA length. 20 bp linker DNA DNs yield the highest FRET efficiency and 50 bp linked at the nucleosomal side opposite of the fluorescent labels the lowest.

Since the amount of reconstituted nucleosomes is small (1–2 pmol), we did not purify the nucleosomes after reconstitution. The consequences for the interpretation of single molecule data will be discussed in the discussion section.

### 3.2. FRET distributions of MNs

Rather than an average FRET value, as determined from the gel, single molecule experiments reveal the distribution of FRET values obtained from individual nucleosomes. We attribute bursts with an uncorrected proximity ratio lower than 0.3 to particles without FRET. This can be either bare DNA or nucleosomes that are partly unwrapped ('open').

At 0 mM salt, 18% of the elementary MNs shows no FRET (figure 5). We observed that an increase of monovalent salt to 100 mM decreases the open population to 11%.

### 3.3. Linker DNA increases DNA breathing

Although DNA breathing has been well established in MNs, it is unclear how extended DNA linkers affect nucleosome dynamics. Mechanical, hydrodynamic and electrostatic properties of DNA will determine the trajectory and dynamics of the linker DNA, which is linked to the nucleosomal DNA. FRET distributions of MNs with 300 bp linker DNA are compared with the distribution of MNs in figure 6. 300 bp of linker DNA attached to the label side causes an increase in the population without FRET from 18 to 26%. When attached to the opposite side, the population without FRET is more than doubled to 40%. Increasing the monovalent salt concentration to 100 mM decreased this effect, indicating that electrostatic repulsion is mainly responsible for enhanced opening of the nucleosome.

### 3.4. DNA breathing is affected by neighboring nucleosomes

While linker DNA has large effects on nucleosome dynamics, it can be expected that the presence of another nucleosome, connected by linker DNA, will further modulate this, as such

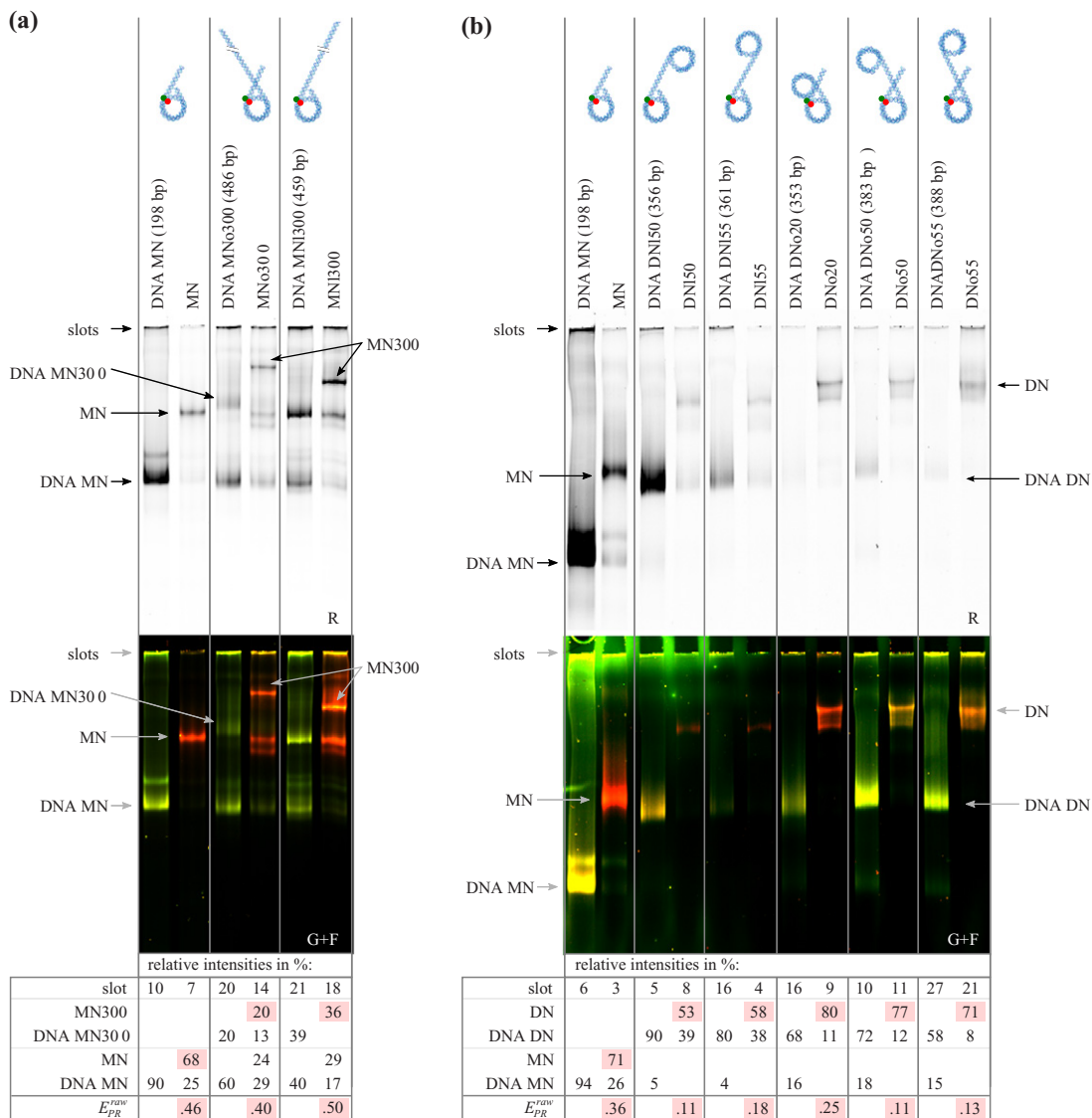


**Figure 4.** Fluorescence images of 5% polyacrylamide gels with reconstituted MNs (a) and DNAs (b). Top (R): acceptor fluorescence upon direct acceptor excitation. Bottom (G + F): false color overlay of donor and acceptor (FRET) fluorescence upon donor excitation. MN: mononucleosome. DN: dinucleosome. Reconstituted nucleosomes show FRET, in contrast to bare DNA. The relative intensities of the bands in each lane from the direct acceptor excitation image are displayed in the table at the bottom, providing a measure for the relative concentrations of the different components (bare DNA, nucleosomes, aggregates). Percentages are approximate within a few percent. For assessment of the fraction of aggregated nucleosomes we included the fluorescence intensities measured at the slot, as quantified in the top row of the table. Numbers corresponding to MN bands are highlighted, and the FRET efficiency calculated from the green and FRET intensities of the bands is indicated in the bottom row.

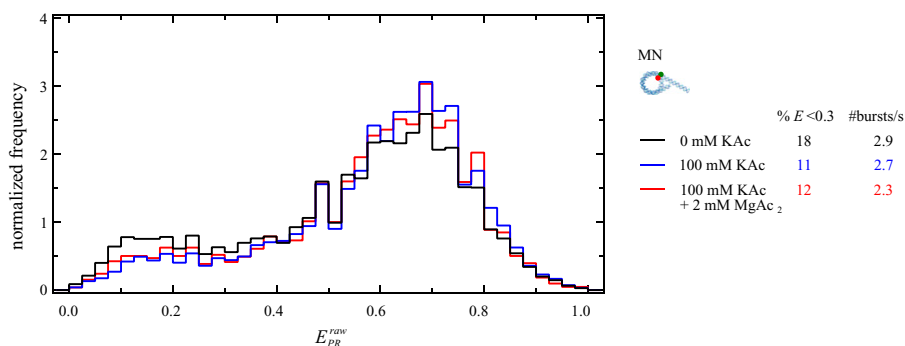


**Figure 5.** FRET efficiency distributions of MNs in different salt conditions. The fraction open nucleosomes decreases from 17 to 11% when increasing the monovalent salt concentration from 0 to 100 mM. Addition of 2 mM magnesium has no effect on the FRET efficiency distribution.

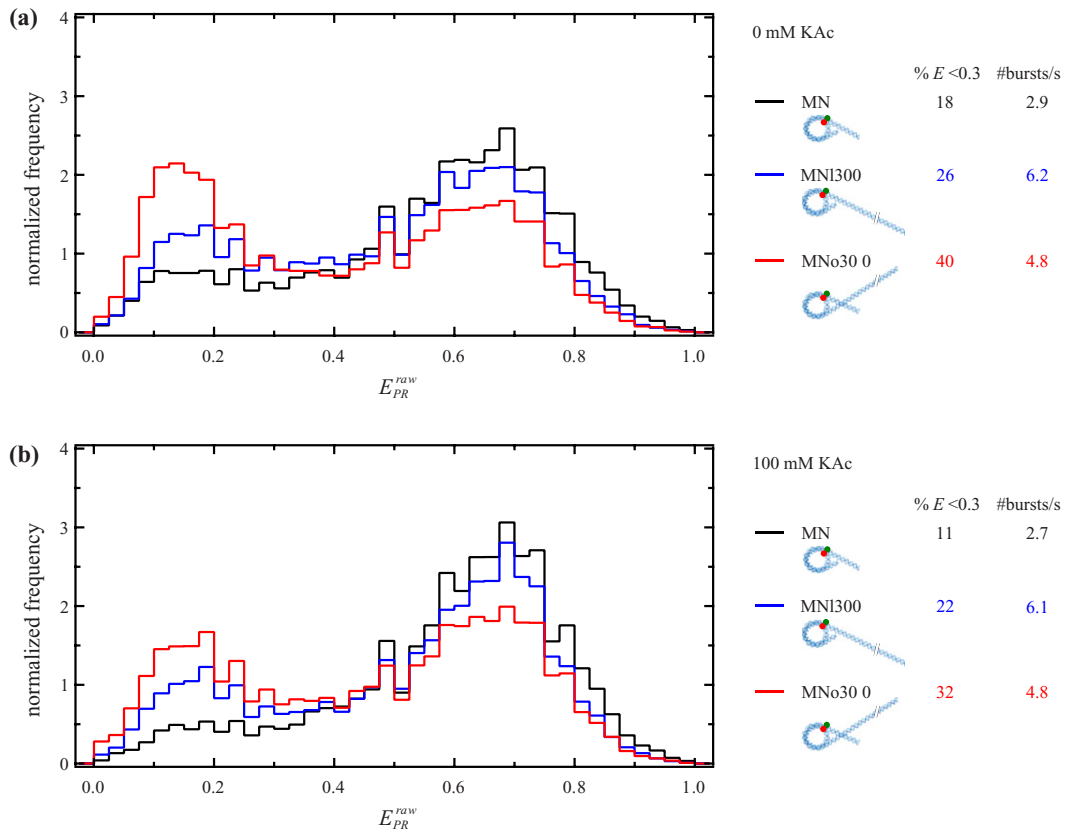


**Figure 6.** FRET efficiency distributions of MNs with 300 bp linker DNA, without (a) and with (b) 100 mM monovalent salt. Nucleosomes with 300 bp linker DNA at the label side (MNI300) or the opposite side (MNNo300) have a larger population of open nucleosomes than nucleosomes without the linker DNA. The linker DNA at the side opposite of the label positions has a surprisingly large effect on the population of open nucleosomes. Adding 100 mM monovalent salt decreases this effect about 25%.

a nucleosome is bulkier and carries a high charge density. All DNs were measured in 100 mM monovalent salt, for proper comparison with the MNs and in accordance with the conditions used for single molecule force spectroscopy on chromatin fibers [18]. Moreover, we included 2 mM  $Mg^{2+}$ , which is required for folding of nucleosomal arrays into dense 30 nm fibers.

### 3.5. DNs with linker DNA at the label side

The distance between non-interacting (straight linker DNA) neighboring nucleosomes with 50 or 55 bp linker DNA is too large for steric or electrostatic effects between the nucleosomes to play a role. Indeed, between the MNs and the DNs with 50 bp linker DNA, there are only minor changes in the FRET distribution (see figure 7). DNs with 55 bp linker DNA, however, show a significantly larger population without FRET. This suggests that a difference in interactions between nucleosomes results in an increased unwrapping probability. We did however not observe an effect of 2 mM magnesium on the FRET distributions.

### 3.6. DNs with linker DNA at the side opposite of the label

When the second nucleosome is attached to the side opposite of the labels, we similarly expect no steric or electrostatic effect between non-interacting nucleosomes. However, as can be

seen in figure 8, DNs with 50 and with 55 bp linker DNA both show a FRET distribution that is different from that of the MN. In these constructs, both interactions between the two nucleosomes, between the linker DNAs, and between nucleosomes and linker DNA may play a role, giving rise to a more complex shape of the distribution, including more pronounced intermediate states.

For the DNs with the linker DNA attached to the side opposite of the fluorescent labels we could also build a construct with 20 bp linker DNA. This distance is too short for the nucleosomes to interact in a face-to-face orientation. The FRET distribution of DNs with 20 bp linker DNA has a slightly increased population with intermediate FRET values as compared to MNs, and a similar low FRET fraction. The close proximity of the nucleosomes ( $\sim 7$  nm linker DNA) could allow interactions between the DNA and/or histone octamers of neighboring nucleosomes which may affect nucleosome breathing.

## 4. Discussion

Here, we showed that the presence of linker DNA and/or a neighboring nucleosome significantly influences nucleosomal DNA dynamics. Constructs of single nucleosomes flanked by long stretches of linker DNA or by neighboring nucleosomes differ in FRET efficiency distribution from MNs flanked by short stretches of linker DNA.

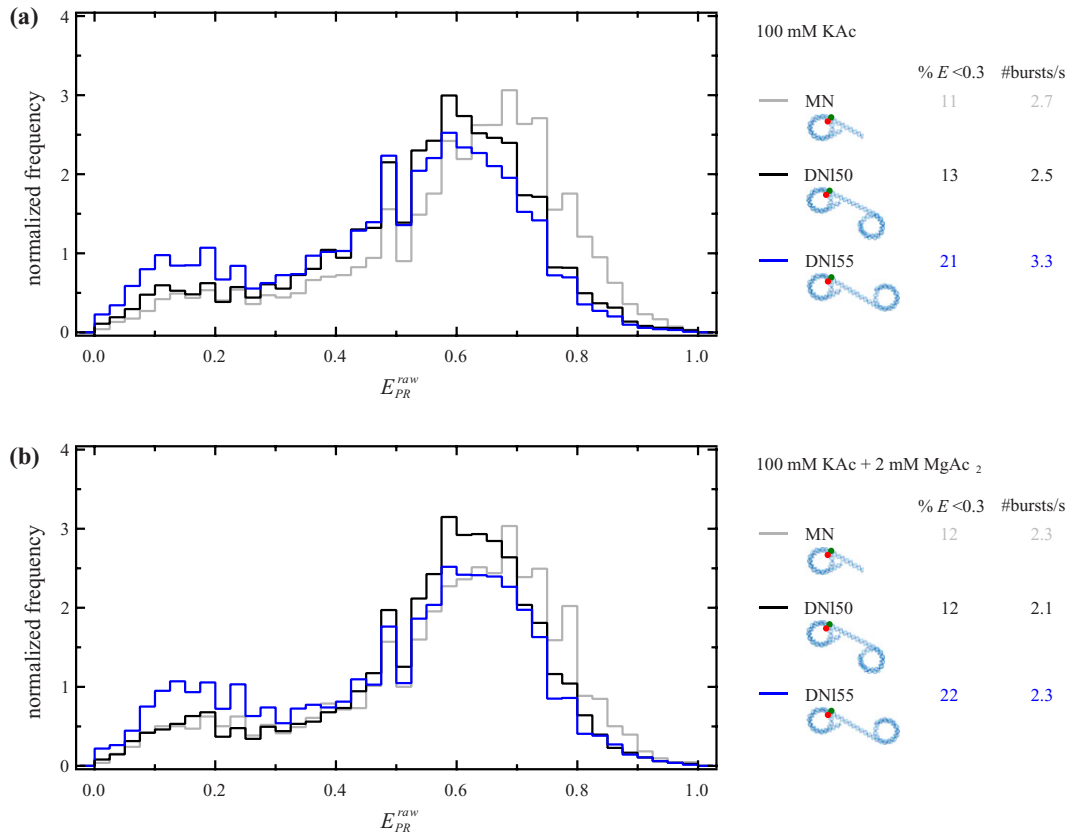


**Figure 7.** FRET efficiency distributions of DN constructs linked via the fluorescent label side with either 50 bp (DNI50) or 55 bp (DNI55) linker DNA, without (a) and with (b) 2 mM magnesium. DN constructs with 50 bp linker DNA show the same distribution as MNs. DN constructs with 55 bp linker DNA on the other hand show a larger population of open nucleosomes. Addition of 2 mM  $Mg^{2+}$  has no visible effect on the FRET efficiency distributions.

#### 4.1. Sample handling

Nucleosomes are known to be very sensitive to concentration, buffer conditions and surface exposure [1, 5, 11, 17]. All FRET efficiency distributions that we report here are the result of multiple measurements, that are reproducible within 5% (fraction  $E_{PR}^{raw} < 0.3$ ). Under suboptimal measurement conditions, e.g. too high dilution and non-passivated surfaces (data not shown), the differences between samples showed the same trend, but generally had a larger fraction of bursts without FRET, indicating that nucleosomes dissociate under these conditions. It is interesting to note that DN constructs appeared to be less susceptible to dilution- and surface- driven dissociation than MNs. This is consistent with cooperative binding of nucleosomes [36].

#### 4.2. Sample heterogeneity

Despite careful titration and the use of the strong 601 nucleosome positioning element, gel electrophoresis shows that the reconstitution yield is in many cases not perfect. For some constructs the percentage of nucleosomes in the sample was only about 30%. Besides nucleosomes, the sample consists of one or more of following components: unconstituted DNA, unligated DNA, nucleosomes on the unligated DNA and aggregates that remained in the slot. Although this heterogeneity in the sample makes quantification

of the results difficult, the qualitative differences between the constructs still hold. The implications for the single molecule data interpretation are described below.

**4.2.1. Mononucleosomes.** Quantification of the band intensities of the gel shown in figure 4 yields  $\sim 70\%$  of reconstituted nucleosomes and  $\sim 25\%$  of unconstituted DNA. A significant amount of the material is left in the slots due to aggregation. In the single molecule experiments however, the fraction without FRET is only 11% (at 100 mM salt), which sets the maximum on the amount of unconstituted DNA. The real amount is probably lower, because this population also consists of partly unwrapped nucleosomes. The amount of free DNA present in the gel, which is more than twice as high as the upper limit that follows from single molecule measurements, is therefore not representative for the reconstitution yield.

Gel electrophoresis can impose severe disruptions on a nucleosome sample. Conditions in the gel, such as low nucleosome concentration, drive nucleosome dissociation, resulting in a larger fraction of free DNA. Hence, we can not equate the reconstitution yield observed in the gel to the amount of unconstituted DNA in the single molecule experiments. The amount of free DNA is however the same in different single molecule experiments of the same sample, i.e. MNs in different salt concentrations. The qualitative decrease of the fraction of open nucleosomes with increasing

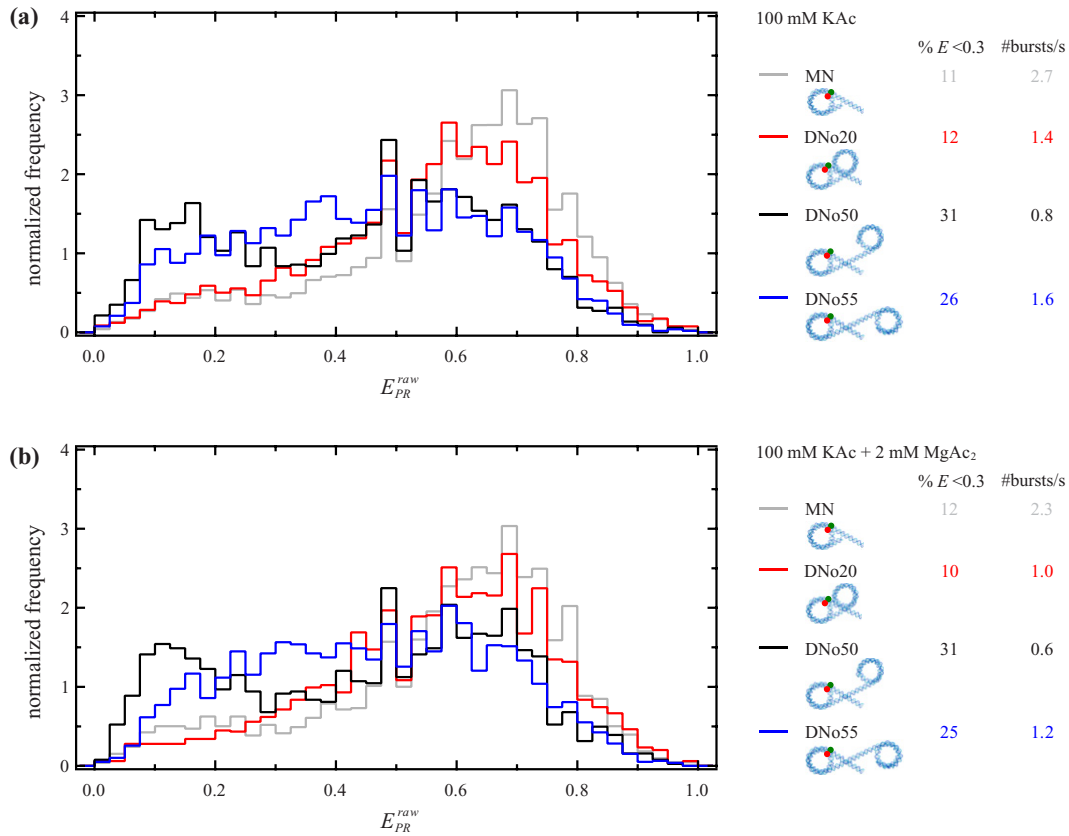


**Figure 8.** FRET efficiency distributions of DN constructs linked via the side opposite of the fluorescent labels with either 20 bp (DNo20), 50 bp (DNo50) or 55 bp (DNo55) linker DNA, without (a) and with (b) 2 mM magnesium. DN constructs with 20 bp linker DNA show a similar distribution to MNs. DN constructs with 50 bp linker DNA show a much larger open population. DN constructs with 55 bp linker DNA also show a much larger open population, and in addition a larger fraction with intermediate FRET efficiencies. Addition of 2 mM  $Mg^{2+}$  has no visible effect on the FRET efficiency distributions.

salt concentration can therefore not be explained by differences in reconstitution yield.

The material left in the slots after gel electrophoresis probably consists of aggregates, and can be as high as 20% or more in some samples. Aggregates can be detected in the single molecule experiments by bursts with increased duration and intensity. Hardly any such signatures of aggregates were found, indicating that the aggregates found in the slots are artifacts due to the gel electrophoresis, or that these aggregates precipitated before the single molecule experiments.

**4.2.2. MNs with linker DNA.** Due to incomplete ligation of the DNA construct, a mixture of MNs with and without 300 bp linker DNA can present in these samples. Figure 4 shows that indeed about half of the nucleosomes lacks the linker. The increase in the fraction of nucleosomes without FRET when 300 bp linker is added is therefore underestimated and the effect of linker DNA on DNA breathing may be larger than measured here.

**4.2.3. Dinucleosomes.** Unreconstituted DNA is present in the polyacrylamide gels of the DN reconstitutions in various amounts. For the DN constructs with the second nucleosome attached to the label side (DNI50 and DNI55), the amount of unreconstituted DNA is as high as  $\sim 40\%$ , while for the DN

with the second nucleosome attached to the side opposite of the labels (DNo20, DNo50 and DNo55), it is only  $\sim 10\%$ . The difference between these sets of constructs could be explained by the concentration difference of the nucleosomes loaded into the gel. Comparison with the no-FRET fraction from single molecule experiments shows that the real fraction of unreconstituted DNA is at most 10% for both sets of constructs, which is comparable to the amount of unreconstituted DNA in the elementary MN. Differences should therefore be attributed to (dynamic) changes in nucleosome conformation.

### 4.3. Linker DNA increases breathing in MNs

The presence of 300 bp linker DNA enhances unwrapping of nucleosomal DNA on both sides of the nucleosome. This could be explained by electrostatic repulsion between the entering and exiting DNA, increasing the unwrapping probability of the nucleosomal DNA. Addition of salt decreases this effect by screening of charges on the DNA. This salt effect was smaller but still measurable in the elementary MN with 39 and 12 bp of linker DNA.

The increase of FRET between 0 and 100 mM KAc is somewhat counterintuitive, regarding that high salt destabilizes nucleosomes: DNA and histone octamers completely dissociate from each other at 2 M [10, 26]. In a recent paper, Gansen *et al* [12], investigated FRET in MNs over a wide

range of nucleosome and salt concentrations. They observed an increase in FRET at moderate salt concentrations as well, but around 400–600 mM. They attribute this to the formation of an intermediate nucleosome conformation towards full dissociation, probably missing one or two dimers. The possibility to observe this intermediate depends on the label positions. With our choice of label positions, at the second bp from the nucleosome exit, dimer loss would result in a complete loss of FRET. We attribute the increase in FRET at 100 mM salt, which is dependent on the length of the linker DNA, to diminished electrostatic repulsion between the linker DNAs. The destabilizing effect of salt on DNA–histone interactions and the electrostatic screening of linker DNAs counteract each other. At modest salt concentrations, the diminished repulsion between linker DNAs apparently dominates over the decreased stability of DNA–histone contacts, resulting in a net increase of the high-FRET population.

#### 4.4. Dinucleosomes

Increased unwrapping due to electrostatic repulsion of the linker DNAs is also observed for DN with 50 bp linker DNA (DNo50), where the no-FRET fraction is increased compared to MNs. DN separated by 55 bp linker DNA, however, have a ~10% larger no-FRET population than with 50 bp linker DNA. Apparently, the neighboring nucleosome increases the unwrapping probability. Interactions between linker DNAs would be the same for both 50 and 55 bp linker DNA. The observed difference in FRET distribution must therefore be attributed to a difference in nucleosome–nucleosome interactions.

Surprisingly, we observe no effect of magnesium in nucleosome–nucleosome interactions. Magnesium is required to induce compaction in nucleosomal arrays with 50 bp linker DNA in [18, 27]. In our DN, we do not observe any change in DNA breathing after addition of magnesium, suggesting that the nucleosome is not constrained differently with or without  $Mg^{2+}$ . Perhaps a DN is a too small unit for mimicking chromatin fiber folding. Magnesium could for example help to bring non-neighboring nucleosomes together, stabilizing two gyres of the ‘super helix’ in the fiber.

To rationalize the FRET distribution of DN with 55 bp linker DNA at the side opposite of the fluorescent labels (DNo55), we need to consider several effects. First, electrostatic repulsion between the linker DNAs favors unwrapping, as for the 50 bp linker DNA construct (DNo50). Second, nucleosome–nucleosome interactions further enhance unwrapping at the side of the linker DNA, similar to the DN with 55 bp linker DNA at the label side (DNI55). If such steric constraints are responsible for increased unwrapping, unwrapping at the side of the linker DNA would be anti-correlated to unwrapping at the opposite side, which is observed as a smaller no-FRET population for DN with 55 bp rather than 50 bp of linker DNA. Third, if nucleosome–nucleosome interactions occur, the electrostatic interactions between the entering and exiting DNA change due to an altered linker DNA trajectory. The interplay between these effects determines the distribution of FRET efficiencies.

An increase in nucleosomes with intermediate FRET was observed for the DN with 55 bp linker DNA attached to the side opposite of the fluorescent labels (DNo55). An intermediate FRET efficiency can result from the average of two conformations when the concentration of labeled nucleosomes in the sample is too high, such that multiple nucleosomes are in the excitation focus at the same time (see [12]). Here, the concentration of labeled nucleosomes is low enough to measure the FRET efficiency in each individual nucleosome separately, as verified by the number of bursts per second. Thus, there must be a fraction of nucleosomes that have a conformation in between open and fully wrapped.

Linker DNA of 20 bp is too short to allow neighboring nucleosomes to interact in a face-to-face manner. The linker DNA and the two nucleosomes are however so close that they are able to interact directly, for example via electrostatic interactions between the DNA and the histone tails. The FRET distribution for DN with 20 bp linker DNA (DNo20) is indeed slightly altered compared to MNs. A small increase in the population with intermediate FRET efficiencies points to a partly unwrapped configuration that is favored, possibly due to interactions between the linker DNA and the neighboring nucleosome.

To probe nucleosome–nucleosome interactions and their dynamics directly, it will be worthwhile to investigate DN with various linker lengths, where one FRET label is located at each of the two nucleosomes at well-chosen positions. High FRET will then correspond to nucleosome–nucleosome interactions. However, this requires detailed insight into the structure of DN, as the small Förster radius imposes strict constraints on the positions of the pair of labels. Only for 20 bp linker DNA has it been possible to do this [23] with the help of the crystal structure [30]. Such higher order folding remains enigmatic for larger linker lengths.

## 5. Conclusions

We performed spFRET experiments on DNA breathing in nucleosomes flanked by linker DNA and/or a neighboring nucleosome. We observed that the presence of linker DNA and a neighboring nucleosome both influence breathing of nucleosomal DNA. Electrostatic repulsion between the entering and exiting DNA favors unwrapping. An increase of the salt concentration reduces the unwrapping probability by screening electrostatic interactions between the linker DNAs.

Like in previous studies, we observed that interactions between neighboring nucleosomes depend on linker length. Here we showed that not only the linker length but also the phasing relative to the pitch of the DNA affects the interaction between neighboring nucleosomes. A linker length of 50 bp does not seem to favor nucleosome–nucleosome interactions, whereas an increase in linker length with only 5 bp results in increased unwrapping of nucleosomal DNA, probably due to nucleosome–nucleosome interactions in such a DN.

The conformation and dynamics of nucleosomal DNA has important implications for the structure and dynamics of chromatin fibers. On one hand, the accessibility of nucleosomal DNA, which has mainly been investigated in

isolated nucleosomes before, depends strongly on chromatin structure. On the other hand, DNA linker length modulates chromatin structure by allowing interactions between direct neighbors only for specific linker lengths. In this study we contributed to the understanding of these phenomena by carefully monitoring the effects that addition of linker DNA and nucleosome neighbors have on DNA breathing.

## Acknowledgments

We thank Guilherme Santos and Professor Dr Daniela Rhodes from the MRC Laboratory of Molecular Biology, Cambridge, UK, for providing the chicken erythrocyte histone octamers and Ineke de Boer-Tuyn for technical support. This work is part of the research program of the Foundation for Fundamental Research on Matter (FOM), which is part of the Netherlands Organization for Scientific Research (NWO).

## References

- [1] Andrews A J and Luger K 2011 Nucleosome structure(s) and stability: variations on a theme *Annu. Rev. Biophys.* **40** 99–117
- [2] Brogaard K, Xi L, Wang J-P and Widom J 2012 A map of nucleosome positions in yeast at base-pair resolution *Nature* **486** 496–501
- [3] Buning R and van Noort J 2010 Single-pair FRET experiments on nucleosome conformational dynamics *Biochimie* **92** 1729–40
- [4] Chien F-T and van Noort J 2009 10 Years of tension on chromatin: results from single molecule force spectroscopy *Curr. Pharm. Biotechnol.* **10** 474–85
- [5] Claudet C, Angelov D, Bouvet P, Dimitrov S and Bednar J 2005 Histone octamer instability under single molecule experiment conditions *J. Biol. Chem.* **280** 19958–65
- [6] Dahan M, Deniz A A, Ha T, Chemla D S, Schultz P G and Weiss S 1999 Ratiometric measurement and identification of single diffusing molecules *Chem. Phys.* **247** 85–106
- [7] Davey C A, Sargent D F, Luger K, Maeder A W and Richmond T J 2002 Solvent mediated interactions in the structure of the nucleosome core particle at 1.9 Å resolution *J. Mol. Biol.* **319** 1097–113
- [8] Deniz A A, Dahan M, Grunwell J R, Ha T, Faulhaber A E, Chemla D S, Weiss S and Schultz P G 1999 Single-pair fluorescence resonance energy transfer on freely diffusing molecules: observation of Förster distance dependence and subpopulations *Proc. Natl Acad. Sci. USA* **96** 3670–5
- [9] Eggeling C, Berger S, Brand L, Fries J R, Schaffer J, Volkmer A and Seidel C A M 2001 Data registration and selective single-molecule analysis using multi-parameter fluorescence detection *J. Biotechnol.* **86** 163–80
- [10] Eickbush T H and Moudrianakis E N 1978 The histone core complex: an octamer assembled by two sets of protein–protein interactions *Biochemistry* **17** 4955–64
- [11] Gansen A, Hauger F, Tóth K and Langowski J 2007 Single-pair fluorescence resonance energy transfer of nucleosomes in free diffusion: optimizing stability and resolution of subpopulations *Anal. Biochem.* **368** 193–204
- [12] Gansen A, Hieb A R, Böhm V, Tóth K and Langowski J 2013 Closing the gap between single molecule and bulk FRET analysis of nucleosomes *Plos One* **8** e57018
- [13] Gansen A, Tóth K, Schwarz N and Langowski J 2009 Structural variability of nucleosomes detected by single-pair Förster resonance energy transfer: histone acetylation, sequence variation, and salt effects *J. Phys. Chem. B* **113** 2604–13
- [14] Ha T, Enderle T, Ogletree D F, Chemla D S, Selvin P R and Weiss S 1996 Probing the interaction between two single molecules: fluorescence resonance energy transfer between a single donor and a single acceptor *Proc. Natl Acad. Sci. USA* **93** 6264–8
- [15] Howell S C, Andresen K, Jimenez-Useche I, Yuan C and Qiu X 2013 Elucidating internucleosome interactions and the roles of histone tails *Biophys. J.* **105** 194–9
- [16] Koopmans W, Buning R, Schmidt T and van Noort J 2009 spFRET using alternating excitation and FCS reveals progressive DNA unwrapping in nucleosomes *Biophys. J.* **97** 195–204
- [17] Koopmans W, Schmidt T and van Noort J 2008 Nucleosome immobilization strategies for single-pair FRET microscopy *Chem. Phys. Chem.* **9** 2002–9
- [18] Kruithof M, Chien F-T, Routh A, Logie C, Rhodes D and van Noort J 2009 Single-molecule force spectroscopy reveals a highly compliant helical folding for the 30 nm chromatin fiber *Nature Struct. Mol. Biol.* **16** 534–40
- [19] Lee N K, Kapanidis A N, Wang Y, Michael X, Mukhopadhyay J, Ebright R H and Weiss S 2005 Accurate FRET measurements within single diffusing biomolecules using alternating-laser excitation *Biophys. J.* **88** 2939–53
- [20] Neumann H, Hancock S M, Buning R, Routh A, Chapman L, Somers J, Owen-Hughes T, van Noort J, Rhodes D and Chin J W 2009 A method for genetically installing site-specific acetylation in recombinant histones defines the effects of H3 K56 acetylation *Mol. Cell* **36** 153–63
- [21] Olins D E and Olins A L 2003 Chromatin history: our view from the bridge *Nature Rev. Mol. Cell Biol.* **4** 809–14
- [22] Poirier M G, Bussiek M, Langowski J and Widom J 2008 Spontaneous access to DNA target sites in folded chromatin fibers *J. Mol. Biol.* **379** 772–86
- [23] Poirier M G, Oh E, Tims H S and Widom J 2009 Dynamics and function of compact nucleosome arrays *Nature Struct. Mol. Biol.* **16** 938–44
- [24] Polach K J and Widom J 1995 Mechanism of protein access to specific DNA sequences in chromatin: a dynamic equilibrium model for gene regulation *J. Mol. Biol.* **254** 130–49
- [25] Prunell A and Kornberg R D 1982 Variable center to center distance of nucleosomes in chromatin *J. Mol. Biol.* **154** 515–23
- [26] Rippe K, Mazurkiewicz J and Kepper N 2008 Interactions of histones with DNA: nucleosome assembly, stability, dynamics, and higher order structure *DNA Interactions with Polymers and Surfactants* ed R Dias and B Lindman (Hoboken, NJ: Wiley) p 135–72
- [27] Robinson P J J, An W, Routh A, Martino F, Chapman L, Roeder R G and Rhodes D 2008 30 nm chromatin fibre decompaction requires both H4-K16 acetylation and linker histone eviction *J. Mol. Biol.* **381** 816–25
- [28] Robinson P J J and Fairall L, Huynh V A T and Rhodes D 2006 EM measurements define the dimensions of the ‘30 nm’ chromatin fiber: evidence for a compact, interdigitated structure *Proc. Natl Acad. Sci. USA* **103** 6506–11
- [29] Routh A, Sandin S and Rhodes D 2008 Nucleosome repeat length and linker histone stoichiometry determine chromatin fiber structure *Proc. Natl Acad. Sci. USA* **105** 8872–7
- [30] Schalch T, Duda S, Sargent D F and Richmond T J 2005 X-ray structure of a tetranucleosome and its implications for the chromatin fibre *Nature* **436** 138–41
- [31] Song F, Chen P, Sun D, Wang M, Dong L, Liang D, Xu R-M, Zhu P and Li G 2014 Cryo-EM study of the chromatin fiber reveals a double helix twisted by tetranucleosomal units *Science* **344** 376–80
- [32] Tims H S, Gurunathan K, Levitus M and Widom J 2011 Dynamics of nucleosome invasion by DNA binding proteins *J. Mol. Biol.* **411** 430–48

- [33] Tóth K, Brun N and Langowski J 2001 Trajectory of nucleosomal linker DNA studied by fluorescence resonance energy transfer *Biochemistry* **40** 6921–8
- [34] Wang J-P, Fondufe-Mittendorf Y, Xi L, Tsai G-F, Segal E and Widom J 2008 Preferentially quantized linker DNA lengths in *saccharomyces cerevisiae* *PLoS Comput. Biol.* **4** e1000175
- [35] Widom J 1992 A relationship between the helical twist of DNA and the ordered positioning of nucleosomes in all eukaryotic cells *Proc. Natl Acad. Sci. USA* **89** 1095–9
- [36] Yodh J G, Lyubchenko Y L and Shlyakhtenko L S, Woodbury N and Lohr D 1999 Evidence for nonrandom behavior in 208–12 subsaturated nucleosomal array populations analyzed by AFM *Biochemistry* **38** 15756–63
- [37] Zheng G, Lu X-J and Olson W K 2009 Web 3DNA—a web server for the analysis, reconstruction, and visualization of three-dimensional nucleic-acid structures *Nucl. Acids Res.* **37** W240–6